

Some recent results on charmonium from ZEUS experiment

P. BELLAN

Università di Padova and INFN, Sezione di Padova - Padova, Italy

(ricevuto il 21 Dicembre 2005; approvato il 13 Marzo 2006; pubblicato online il 9 Giugno 2006)

Summary. — Various results obtained by the ZEUS Collaboration concerning J/ψ mesons are reported, either in regime of photoproduction or in deep inelastic scattering. The measurements are compared with the available theoretical models and with the predictions of the k_T -factorisation as well as of the CASCADE event generator, searching to understand the role of the color singlet and colour octet contributions in the charmonium production.

PACS 12.39.Jh – Nonrelativistic quark model.

PACS 12.39.Hg – Heavy quark effective theory.

PACS 13.20.-v – Leptonic, semileptonic, and radiative decays of mesons.

PACS 13.20.Fc – Decays of charmed mesons.

PACS 13.20.Gd – Decays of J/ψ , Υ , and other quarkonia.

1. – Contest between theoretical and experimental results

The different measurements carried out from the ZEUS⁽¹⁾ Collaboration concerning J/ψ mesons, namely the cross-sections differential in p_T and z , either in PHP and DIS regime, and the studies of the J/ψ helicity distributions in PHP will be compared with the theoretical prediction currently available.

Furthermore, the comparison with the experimental data will be used as a test of reliability of a new kind of Monte Carlo events generator, the CASCADE MC.

After a short description of the main processes taking place in ep collision and the variables useful to describe them, we will move to briefly expose the theoretical background from which the predictions come, as well as the ingredients with which the CASCADE event generator is built. Finally the experimental results will be presented together to the theoretical prediction, and some speculation about the role of different production mechanism will be attempted.

In all the studies reported here the reconstructed decay channel of the J/ψ mesons is always $J/\psi \rightarrow \mu^+\mu^-$. Muon identification is mainly performed by finding tracks

⁽¹⁾ A detailed description of the ZEUS detector can be found in [1].

in the barrel and rear muon chambers⁽²⁾ or minimum-ionising energy deposits in the calorimeter, matched to track segments in the central wire drift chamber.

2. – Formal tools

To introduce the main kinematic variables useful to describe a generic ep collision and the vector mesons production in inclusive reactions, let us start considering the process

$$(1) \quad e(k) p(P) \rightarrow e(k') X(P^X),$$

where the initial and final particles quadrimomenta are indicated in parenthesis. To describe the leptonic vertex $e\text{-}\gamma$ one introduces the following kinematic variables:

$$(2) \quad s \equiv (P + k)^2 \quad y \equiv \frac{P \cdot q}{P \cdot k}, \quad Q^2 \equiv -q^2 \equiv -(k - k')^2,$$

where s is the energy square in the center-of-mass frame ep and Q^2 is the opposite of the square of the vector boson quadrimomentum exchanged between the leptonic and the hadronic vertex, also called *virtuality*. The physical meaning of the y variable will be illustrated in the following. The inclusive J/ψ production in the electron-proton collisions through a virtual photon, γ^* ⁽³⁾, corresponds to the process

$$(3) \quad e(k) p(P) \rightarrow e(k') J/\psi(p^{J/\psi}) X(P^X),$$

where the final state consists of the scattered electron, a J/ψ and a generic hadronic system X . The hadronic sub-process $\gamma^* p \rightarrow J/\psi X$ is characterised by

$$(4) \quad W_{\gamma p}^2 \equiv (P + q)^2 = (p^{J/\psi} + P^X)^2, \quad z^{J/\psi} \equiv \frac{P \cdot p^{J/\psi}}{P \cdot q},$$

$$(5) \quad t \equiv (q - p^{J/\psi})^2 = (P^X - P)^2, \quad M_X^2 \equiv (P^X)^2,$$

where $W_{\gamma p}$ is the energy in the $\gamma^* p$ center of mass, t is the squared quadrimomentum lost by the incident proton and M_X is the invariant mass of the hadronic final state X excluding the J/ψ . Another very important variable is the meson transverse momentum with respect to γ^* axis, p_T . Let us call $E_e(E'_e)$ the incident (scattered) electron energy, $E_{J/\psi}$ the J/ψ energy and E_{γ^*} the γ^* energy; so in the proton rest frame we can write

$$(6) \quad y = \frac{E_{\gamma^*}}{E_e}, \quad z^{J/\psi} = \frac{E_{J/\psi}}{E_{\gamma^*}} = \frac{(E - p_z)_{J/\psi}}{(E - p_z)_{\text{hadrons}}}.$$

Therefore the y variable corresponds to the incident electron energy transferred to the photon γ^* , while the $z^{J/\psi}$ variable, called *inelasticity*, corresponds to the virtual photon energy transferred to the J/ψ .

⁽²⁾ The B/RMUON detector [2].

⁽³⁾ When the γp center-of-mass energy is near the m_{Z^0} threshold, also a virtual Z^0 might be exchanged in the collision, but only when $Q^2 \sim M_{Z^0}^2$ its contribution is comparable with that one of a γ^* exchange.

3. – Processes: classification and terminology

When the proton interacts with a real photon (*i.e.* $Q^2 = 0$) the process is called *photoproduction* (PHP), and the degrees of freedom decrease by one unit, whereas in a deep inelastic scattering (DIS) event the exchanged photon has a nonzero virtuality $Q^2 = -q^2$. Sometimes they refer to a DIS also as *leptoproduction*.

In addition to the reconstructed value of Q^2 , from the experimental point of view what practically distinguishes DIS event from an event in the photoproduction regime is if the electron is detected or not inside the detector after the collision. When the electron in the final state is missing and the Q^2 is very low⁽⁴⁾ we are dealing with an event of photoproduction; for DIS processes, like $e + p \rightarrow e + J/\psi + X$, the electron scattering angle is large enough for the electron to be detected and it does not escape in the rear beam pipe.

3.1. *Where the hadrons come from.* – The photon-proton cross-section may be written as a sum of a *direct*- and a *resolved*-photon contribution. Nevertheless it is important to keep in mind that the separation of direct and resolved reactions is ambiguous beyond LO and only the sum is meaningful⁽⁵⁾.

3.2. *Coloured propagators.* – The most important γ^* - p inelastic channel is the so-called *photon-gluon fusion*, in which the photon interacts with a gluon from the proton producing a coloured $c\bar{c}$ couple. A gluon emitted from the $c\bar{c}$ couple guarantees the colour neutrality of the vector meson. Then in the *resolved photon* process, in which the hard sub-processes that take places can be $g g \rightarrow g V$, $g g \rightarrow \gamma g$, where V indicates the produced vector meson: a J/ψ , a $\psi(2S)$ or a χ state. χ are possible secondary sources of J/ψ through radiative decays. One refers to *feeddown* when the J/ψ mesons are produced by the cascade decay of others particles as the upper excited charmonia states. At high Q^2 also the b quark decay can contribute; in this case the J/ψ is not spatially isolated from the hadronic final system.

4. – Reality vs. theory

Inelastic production of charmonium can be described in two steps:

1. the creation of a $c\bar{c}$ quark pair, calculable in the perturbative QCD framework;
2. the formation of the bound state, occurring at long distances and described by phenomenological models.

The energy-momentum scale appearing in both heavy-quarkonium annihilation decays and hard-scattering production is the heavy-quark mass m_Q , which is much larger than Λ_{QCD} ⁽⁶⁾. But even if the associated values of the QCD running coupling constant are much less than one ($\alpha_s(m_c) \approx 0.25$), in order to make use of perturbative methods one must first separate the short-distance/high-momentum perturbative effects of the hard momentum scale $\sim m_Q$, from the long-distance/low-momentum, nonperturbative effects

⁽⁴⁾ The cut usually applied is $Q^2 < 1$ GeV.

⁽⁵⁾ The factorization scale related to the subtraction of divergences in the collinear partons emission from the incoming photon appears in both the direct and the resolved contributions.

⁽⁶⁾ In the case of production, also the transverse momentum p_T can be much larger than Λ_{QCD} .

of the soft momentum scale $\sim \Lambda_{\text{QCD}}$, related to the dynamics of the quarkonium bound state. One refers to this approach as the *(topological) factorization*.

A convenient way to carry out this separation is through the use of an effective field theory as the Nonrelativistic QCD.

4.1. NRQCD, factorisation and neighbourhood. – NRQCD reproduces full QCD accurately at momentum scales of order mv and smaller, where v is the typical heavy-quark velocity in the bound state in the CM frame. The inclusive cross-section for the direct production of the quarkonium H at large transverse momentum ($p_T \gtrsim m_Q$) in hadron or ep colliders can be written as a sum of products of NRQCD matrix elements and short-distance coefficients:

$$(7) \quad \sigma[H] = \sum_n \sigma_n(\Lambda) \langle \mathcal{O}_n^H(\Lambda) \rangle.$$

Here σ_n are the short-distance coefficients, $\langle \mathcal{O}_n^H \rangle$ are vacuum expectation values of four-fermion operators in NRQCD, n denotes collectively the colour and angular quantum numbers and Λ is the ultraviolet cut-off of the effective theory. There is a formula analogous to eq. (7) for inclusive quarkonium annihilation rates, except that the vacuum-to-vacuum matrix elements are replaced by quarkonium-to-quarkonium matrix elements.

4.2. What we are able to compute... more or less. – The short-distance coefficients $\sigma_n(\Lambda)$ in eq. (7) are the (process-dependent) partonic cross-sections⁽⁷⁾ to make a $Q\bar{Q}$ pair in a given quantum state and with small relative momentum. The $Q\bar{Q}$ pair can be produced with a nonzero value of orbital angular momentum, as a spin singlet or triplet but also in a *colour-singlet* or in a *colour-octet* state. The colour and angular-momentum quantum numbers n of the intermediate $Q\bar{Q}$ pair do not need be equal those of the physical quarkonium H : soft gluons can be emitted before the bound state is formed and change the colour and spin of the heavy-quark pair; their effects end in the long-distance matrix elements. Such a possibility is ignored in the colour-singlet model (CSM), where one assumes that only heavy-quark pairs produced in the dominant Fock state form a physical quarkonium. The short-distance coefficients are determined by matching the square of the production amplitude in NRQCD to full QCD and this matching can be carried out in perturbation theory in an usual expansion in strong coupling α_s .

4.3. What we have to learn from the experiment. – The non-perturbative transition probabilities from the $Q\bar{Q}$ state into the quarkonium are given by vacuum expectation values of local four-fermion operators in NRQCD, corresponding to the evolution into a colour-singlet quarkonium of a $Q\bar{Q}$ pair created at short distance in a colour singlet state or octet state. In the case of decay, the colour-octet matrix elements have the interpretation of the probability to find the quarkonium in a Fock state consisting of a $Q\bar{Q}$ pair plus some number of gluons. Currently, the matrix elements governing the strength of this process cannot be calculated, and have to be extracted from the data. These matrix elements are somewhat analogous to parton fragmentation functions. They are expected to be universal, *i.e.* process independent, so the comparison between the values extracted from ψ ⁽⁸⁾ cross-section measurements obtained in different environments constitutes a stringent test of this approach.

⁽⁷⁾ Convolved with parton distributions if there are hadrons in the initial state.

⁽⁸⁾ Here and in the following, with ψ we refer to J/ψ or ψ' indifferently.

4.4. *Again separating...* – The NRQCD power counting rules predict a hierarchy among the matrix elements $\langle \mathcal{O}_n^H(\Lambda) \rangle$ in terms of their dependence on the intrinsic heavy-quark relative momentum v . Expanding the hard scattering part of the amplitude in eq. (7) in powers of v and truncating at a given order in v , one can reduce the number of independent matrix elements that contribute to the production cross-section. The simplest truncation of the NRQCD expansion includes four independent matrix elements for each S -wave multiplet (one colour-singlet and three colour-octet) and two independent NRQCD matrix elements for each P -wave multiplet (one colour-singlet and one colour-octet). We will refer to this truncation as the *standard truncation* in v .

It is important to keep in mind the standard NRQCD power counting rules have been derived assuming $m_Q v \gg m_Q v^2 \approx \Lambda_{\text{QCD}}$ and $\alpha_s(m_Q v) \sim v$ ($v^2 \approx 0.3$ for charmonium, and $v^2 \approx 0.1$ for bottomonium). Such a hierarchy is likely to be realized for bottomonium states where $m_Q \approx 5$ GeV. It is, however, not obvious *a priori* that it can be applied to the charmonium system where $m_Q \approx 1.5$ GeV so that $m_Q v \approx 820$ MeV. Depending on the relation between the low energy scales $m_Q v$, $m_Q v^2$ and Λ_{QCD} , alternative power counting schemes may be more appropriate for charmonium. One can try to discriminate them in comparing the various theoretical predictions with the data.

4.5. *CS and CO contributions at HERA.* – The production of J/ψ mesons in ep collisions at HERA is sensitive to both CS and CO contributions. The CS mechanism is expected to be the dominant contribution at intermediate values of the inelasticity variable, $z \lesssim 0.7$, whereas CO mechanism is expected to be dominant at high z .

5. – Why we really need the colour octet states?

The most deep theoretical evidence for the incompleteness of the colour-singlet model comes from the presence of infrared divergences in the production cross-sections and decay rates of P -wave quarkonium at NLO. These divergences cannot be factored into the radial wave function at the origin square absolute value and require that an infrared cut-off to be introduced. But in the NRQCD approach the infrared divergence is cancelled by matching infrared singularity from the radiative corrections to the colour-octet matrix element. In fact, according to the power counting rules, the colour-octet term must be tacked into account, since it scale with the same power of v .

Colour-octet contributions are needed for a consistent description of P -wave quarkonia, but they can be even more important phenomenologically for S -wave states like J/ψ or ψ' : in spite of the NRQCD power counting rules, that said all CO matrix elements for the production (or decay) of S -wave quarkonia are suppressed by powers of the velocity compared to the CS contribution, CO processes can become significant, and even dominant, if the short-distance cross-section for producing $Q\bar{Q}$ in a colour-octet state is enhanced.

Otherwise, from the experimental point of view, the evidence that something else beyond the CS approach there must to be, clearly appeared early, when in the production of ψ mesons measured in $p\bar{p}$ collisions by the CDF Collaboration [3] was evident that predictions of the CS model underestimate the data by factors of between 10 and 80.

6. – Something else to compare with data

Multiple gluon emission can be very important for transverse momentum distributions. Several methods as *resummation*, *Parton-Shower Monte Carlo*, *k_T -factorisation*

and k_T -smearing have been developed to take into account this process.

6.1. Gluons emission. – The k_T -factorisation method is an attempt to take into account initial-state radiation through parton distributions that depend on the parton's transverse momentum k_T as well as on the parton's longitudinal momentum fraction x . It generally gives answers very different from those of collinear factorisation. In the k_T -factorisation approach the J/ψ production process is factorized into a k_T -dependent gluon density and a matrix element for off-shell partons. A LO calculation within this approach is implemented in the Monte Carlo generator CASCADE.

6.2. The event generator. – CASCADE MC incorporates the off-shell matrix elements for the photon-gluon fusion process at LO. The initial-state parton shower is generated according to the CCFM evolution equations. The J/ψ mesons were produced in the framework of the CSM. The gluon density, unintegrated in transverse momentum k_T , was obtained from an analysis of the proton structure functions based on the CCFM equations. In CASCADE the hadronisation was performed with the Lund string model.

7. – Measurements of J/ψ in photoproduction

Quarkonium production in high-energy ep collision is dominated by photoproduction events. Experimental results have been reported for J/ψ and $\psi(2S)$ PHP in a wide kinematical region, $30 \lesssim \sqrt{s_{\gamma p}} \lesssim 200$ GeV. The cross-section is dominated by photon-gluon fusion processes. HERA data have shown that the diffractive process populates the high- z region, $z > 0.9$. The direct and resolved photon processes are expected to dominate in the regions $0.2 \lesssim z < 0.9$ and $z \lesssim 0.2$, respectively. Higher-twist phenomena like elastic/diffractive quarkonium production are not included in the leading-twist calculation of NRQCD and have to be eliminated by either a cut in the J/ψ transverse momentum $p_T \gtrsim 1$ GeV, (but a stronger cut can be assessed more suitable) or by a cut in the J/ψ inelasticity z . Moreover, LO matrix element computed in the CSM for the photon-gluon fusion is singular at $p_T = 0$ and $z = 1$.

At leading order in the velocity expansion, the J/ψ is produced through the colour-singlet channel. Relativistic corrections at $\mathcal{O}(v^2)$ modify the large- z and small- p_T region but can be neglected for $p_T \gtrsim 1$ GeV. The next-to-leading order QCD corrections to the direct photon process increase the cross-section prediction significantly, in particular at $p_T \gtrsim m_c$. At $\mathcal{O}(v^4)$ relative to the colour-singlet contribution, the J/ψ can also be produced through intermediate colour-octet $^3S_1, ^1S_0$ and 3P_J configurations.

The importance of the colour-octet production processes follows from a kinematical enhancement of the short-distance cross-section: $c\bar{c} [8, ^1S_0]$ and $c\bar{c} [8, ^3P_J]$ processes can be produced through t-channel gluon exchange already at lowest order in α_s . The $c\bar{c} [8, ^3S_1]$ -channel is insignificant for the direct-photon contribution, but dominates in resolved-photon interactions at high transverse momentum $p_T \gtrsim 5$ GeV, because it includes a gluon fragmentation⁽⁹⁾ component. This leads to a potentially significant colour-octet contribution, in particular in the large- z region; the size of the effect, however, is difficult to quantify given the substantial uncertainties in the values of the relative matrix elements.

⁽⁹⁾ A process in which the quarkonium is formed in the hadronization of a gluon that is created with even larger transverse momentum.

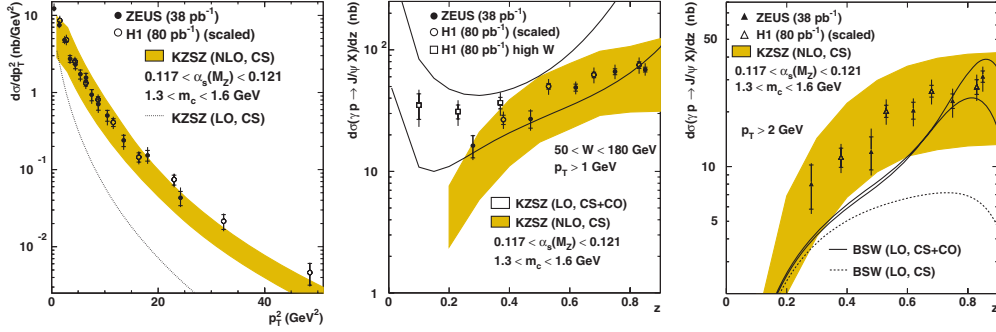


Fig. 1. – Left: J/ψ differential cross-section $d\sigma/dp_T^2$ for $50 < W < 180$ GeV and $0.4 < z < 0.9$. The dotted line represents the LO prediction KZSZ (LO, CS). Center: Differential cross-section $d\sigma/dz$ for $50 < W < 180$ GeV and $p_T > 1$ GeV. The solid lines show the prediction of the KZSZ (LO, CS+CO), calculation performed including both direct and resolved photon processes. The spread in the predictions is due to uncertainties in the extraction of the CO matrix elements. Right: Differential cross-section $d\sigma/dz$ for $50 < W_{\gamma p} < 180$ GeV, $0.1 < z < 0.9$ and $p_T > 2$ GeV, compared with the direct photon LO (CS+CO) calculation from BSW (see the text); the spread in the predictions is due to theoretical uncertainty on the value of the shape-function parameter. The contribution coming only from CS processes is also shown. In all the graphics, the shaded band shows the prediction KZSZ (NLO, CS), including only the direct photon process. The spread in the prediction is due to uncertainties on the charm-quark mass and on the QCD scale parameter, Λ_{QCD} ; a 15% contribution has been added to the predictions to account for the ψ' feeddown. In the data points, the inner error bars show the statistical uncertainty; the outer bars show the statistical and systematic uncertainties added in quadrature.

The theoretical predictions are compared to experimental results obtained by the H1 [4] and ZEUS [5] Collaborations at HERA in fig. 1. Kinematic cuts were introduced to remove the beam-gas interaction, cosmic-ray events and ψ mesons elastically produced; the data were corrected bin by bin for geometric acceptance, detector, trigger and reconstruction efficiencies, as well as for detector resolution. The combinatorial background was estimated by fitting the invariant-mass distribution outside the ψ mass range, where diffractive processes contamination, sizable at low p_T and high z , was estimated by fitting the relative fractions of HERWIG and EPSOFT MC event samples to the data.

Concerning the theoretical prediction therein, the LO calculation from Krämer *et al.* (KZSZ (LO, CS+CO)) includes the CO contributions from both direct and resolved photon processes. The CO matrix elements were extracted by fitting the cross-section $d\sigma/dp_T^2$ for prompt J/ψ production measured by CDF. The matrix elements for the hard subprocesses were computed at LO, while the CO matrix elements were corrected for initial- and final-state gluon radiation by a Monte Carlo technique. The calculation has been extended to include predictions of the J/ψ helicity-angle distributions (BKV (LO, CS)).

The NLO corrections to the direct photon process in the CS calculation are shown only for $p_T > 1$ GeV, since they are no more reliable in the limit $p_T \rightarrow 0$ GeV. The uncertainty regards mainly the input of nonperturbative parameters as m_c and Λ_{QCD} rather than the renormalisation and factorisation scales.

In fig. 1 we can see that the next-to-leading order QCD corrections are crucial to de-

scribe the shape of the J/ψ transverse momentum distribution: once higher-order QCD corrections are included and considering the normalisation uncertainty due to the choice for the charm quark mass and the QCD coupling, the data are adequately described by the colour-singlet channel alone. On the contrary the LO CSM prediction underestimates the data by a factor of 2 to 20 at high p_T . The NLO colour-singlet cross-section includes processes like $\gamma + g \rightarrow Q\bar{Q} [1, {}^3S_1] + g + g$ which are dominated by t-channel gluon exchange and scale as $\sim \alpha_s^3 m_Q^2 / p_T^6$. At $p_T \gtrsim m_Q$ their contribution is enhanced with respect to the leading-order cross-section, which scales as $\sim \alpha_s^2 / m_Q^4 p_T^8$. The same conclusion holds for the J/ψ energy spectrum, *i.e.* the differential cross-section as a function of z , which is particularly sensitive to probe the different production mechanisms. Colour-octet processes are predicted to contribute significantly near the upper and lower endpoint of the energy spectrum. However as we can see in the central plot of fig. 1, the colour-octet enhancement in the high- z region is not supported by the data. However one cannot put stringent constraints on the colour-octet matrix of the 1S_0 and 3P_0 wave (or point towards an inconsistency with the values obtained for the matrix elements from other processes) because the peaked shape of the z -distribution is derived neglecting the energy transfer of soft parton emission in the non-perturbative transition of the colour-octet charm quark pairs. Such kinematic effects, important near the endpoint of the J/ψ energy spectrum, need a summation of singular higher-order terms in the velocity expansion. This is performed at LO by Beneke, Schuler and Wolf (BSW (LO, CS+CO)), where tunable *shape functions* resum an infinite class of CO contributions necessary to predict the shape of the z -distribution in the region $z \gtrsim 0.7$. These functions are responsible for the decrease of the CO contributions towards $z = 1$, due to the lack of phase space for gluon radiation⁽¹⁰⁾. Only the direct photon processes for the CS and CO contributions are included and the CO matrix elements were extracted from measurements by the CLEO Collaboration⁽¹¹⁾. In the right plot of fig. 1 this calculation is compared with the data from both H1 and ZEUS Collaborations; it can be seen that actually the agreement at high z is effectively improved. Keep in mind that the overall shape of the spectrum is weakly dependent on the CO matrix elements, which primarily affect the global normalisation of the spectrum.

8. – Gaining auspices from the muons’s fly

Many of the largest uncertainties in the theoretical predictions, as well as some of the experimental uncertainties, cancel in the cross-sections ratio. Examples in charmonium production are the ratio of the inclusive cross-sections for $\psi(2S)$ and J/ψ production, measured by ZEUS Collaboration [5] and found to be independent of the kinematic variables z , p_T and W , as expected if the underlying production mechanisms for the J/ψ and the ψ' were the same.

Another set of observables in which many of the uncertainties cancel out consists of polarization variables, which can be defined as ratios of cross-sections for the production of different spin states of the same quarkonium. The polarization of the J/ψ meson is expected to differ in the various theoretical approaches discussed here and could in princi-

⁽¹⁰⁾ This treatment introduces an additional parameter into the model, the *shape-function parameter*, which was varied in the range 300–500 MeV based on the CLEO data.

⁽¹¹⁾ From the B meson decays to J/ψ ; the matrix elements extracted from CLEO and CDF are consistent.

ple be used to distinguish between them. Furthermore, helicity studies are mainly shape measurements; consequently, compared with measurements of differential cross-sections, they are less sensitive to the choice of the non-perturbative QCD input parameters such as the charm quark mass or the QCD scale parameter Λ . Moreover, in such a shape measurement, higher-order corrections are not expected to change the theoretical picture very significantly. The standard truncation in v leads to unambiguous predictions for the ratios of production rates of different spin states: for the S -wave charmonium multiplet consisting of J/ψ and η_c , one can take the four independent matrix elements to be $\langle \mathcal{O}_1^{J/\psi}({}^3S_1) \rangle$, $\langle \mathcal{O}_8^{J/\psi}({}^1S_0) \rangle$, $\langle \mathcal{O}_8^{J/\psi}({}^3S_1) \rangle$, and $\langle \mathcal{O}_8^{J/\psi}({}^3P_0) \rangle$. Their relative orders in v are v^0 , v^3 , v^4 , and v^4 , respectively⁽¹²⁾. These four independent matrix elements can be used to calculate the cross-sections for each of the 3 spin states of the J/ψ and then to obtain predictions for the J/ψ polarization.

The angular distribution of the decay products of the quarkonium depends on its spin state. The polarization of a 1^{--} state such as the J/ψ , can be measured from the angular distribution of its decay to leptons.

The helicity analysis was performed from the ZEUS Collaboration [6] in the so-called target frame⁽¹³⁾, where the general decay angular distribution can be parametrised as

$$(8) \quad \frac{d\Gamma(J/\psi \rightarrow l^+l^-)}{d\Omega} \propto 1 + \lambda \cos^2 \theta + \mu \sin 2\theta \cos \phi + \frac{\nu}{2} \sin^2 \theta \cos 2\phi;$$

θ and ϕ are to the polar and azimuthal angle of the l^+ three-momentum *w.r.t* a coordinate system that is defined in the J/ψ rest frame. The parameters λ, μ, ν can be calculated within NRQCD or the CSM as a function of the kinematic variables, such as z and $p_T(J/\psi)$. Integrating in φ and θ the angular distribution becomes, respectively,

$$(9) \quad \frac{1}{\sigma} \frac{d\sigma}{d \cos \theta dy} \propto 1 + \lambda(y) \cos^2 \theta, \quad \frac{1}{\sigma} \frac{d\sigma}{d\varphi dy} \propto 1 + \frac{\lambda(y)}{3} + \frac{\nu(y)}{3} \cos 2\varphi,$$

where the variable y can be either the p_T or the inelasticity z of the J/ψ . The NRQCD factorization approach gives a simple prediction for the polarization variable λ at very large transverse momentum. The production of a quarkonium with $p_T \gg m_{Q\bar{Q}}$ is dominated by gluon fragmentation and NRQCD predicts as the dominant process the gluon fragmentation into a $Q\bar{Q}$ pair in a colour-octet 3S_1 state. The fragmentation probability for this process is of order α_s , while the fragmentation probabilities for all other processes are of order α_s^2 or higher. The NRQCD matrix element for this fragmentation process is $\langle \mathcal{O}[8, {}^3S_1] \rangle$. At large p_T , the fragmenting gluon is nearly on its mass shell, and so is transversely polarized.

Furthermore, the velocity-scaling rules predict that the colour-octet $Q\bar{Q}$ state retains the transverse polarization as it evolves into an S -wave quarkonium state, up to corrections of relative order v^2 . Radiative corrections and colour-singlet production dilute the quarkonium polarization somewhat. Despite of this and of the polarization dilution coming from the feeddown from higher quarkonium states⁽¹⁴⁾ and from spin-flip processes,

⁽¹²⁾ Many observables are sensitive only to the linear combination of two colour-octet ME.

⁽¹³⁾ The quantisation axis z is chosen along the opposite of the incoming proton direction in the J/ψ rest frame. The polar angle θ is defined as the angle between the μ^+ vector in the J/ψ rest frame and the quantisation axis. Azimuthal angle φ is defined *w.r.t.* the y -axis, chosen along the vector $\vec{p}_\gamma \times (-\vec{p}_p)$ in the J/ψ rest frame. Then the x -axis is chosen to complete a right-handed coordinate system.

⁽¹⁴⁾ Feeddown from χ_c and $\psi(2S)$ states is respectively about 30% and 10% of the J/ψ sample.

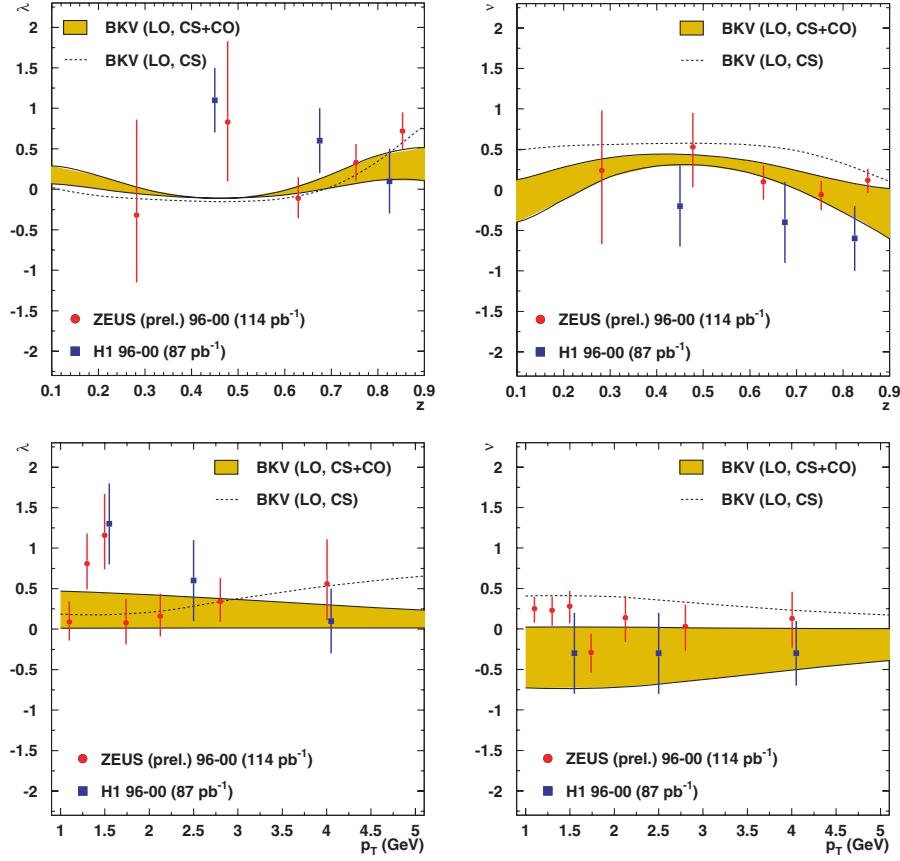


Fig. 2. – Polarization parameters λ (left panels) and ν (right panels) in the target rest frame as functions of z (top panels) and p_T (bottom panels). The error bars on the data points correspond to the total experimental error. The theoretical calculations shown are from the NRQCD approach (shaded bands) with colour-octet and colour-singlet contributions, while the curves show the result from the colour-singlet contribution separately.

a substantial polarization is expected at large p_T , and its detection would be a “smoking gun” for the presence of the colour-octet production mechanism⁽¹⁵⁾.

In fig. 2, the data are shown, together with the band of the BKV (LO, CS+CO) prediction including both CS and CO terms and the corresponding prediction in the restricted CS framework(LO, CS+CO).

An available calculation with the k_T -factorization approach and off-shell gluons predicts that λ should become increasingly negative toward larger values of p_T , whereas in the analysed range of p_T none of the NRQCD calculations predicts a decrease in λ with increasing z . Concerning the ν parameter, all data points are systematically below the prediction of CS alone.

The data are well reproduced by both CS and full NRQCD calculation; however,

⁽¹⁵⁾ In contrast, the colour-evaporation model predicts zero quarkonium polarization.

at present, the errors in the data preclude any firm conclusions. The error band in fig. 2 reproduces the total experimental uncertainties; the error coming from the χ^2 fit procedure is larger *w.r.t.* the systematic uncertainties.

The measurements of the J/ψ polarization as a function of p_T seem to be against the prediction of a polarization increasing at higher values of p_T ⁽¹⁶⁾; however the experimental errors are still too large to conclude. The polarization is probably not strongly affected by multiple gluon emission. Uncertainties from contributions of higher-order in α_s could conceivably change the rates for the various spin states by a factor of two. Therefore it is reasonable to expect an important improvement of the prediction power when the NLO calculation will be carried out, as in the case of PHP.

9. – J/ψ production in deep inelastic scattering

Leptoproduction of quarkonium has been extensively studied in the context of the colour-singlet model and in the framework of the NRQCD factorisation approach including colour-octet processes. With respect to the photoproduction events, at large photon virtualities Q^2 one has:

- grater CO contributions;
- both CS and CO theoretical prediction under better control (the higher the interaction scale, the smaller higher-order and higher-twist corrections);
- lower contamination from diffractive processes (expected to be suppressed at $Q^2 \gg 4m_Q^2$) and from ψ' feeddown;
- γ -resolved processes negligible;
- better experimental efficiency, coming from the scattered electron detection;
- *but* smaller cross-section and hence statistics.

The leading-order J/ψ production process is $\mathcal{O}(\alpha\alpha_s)$ and proceeds purely through intermediate 1S_0 and 3P_J colour-octet configurations. The leptoproduction cross-section in the high-energy limit $Q^2, s \gg 4m_c^2$ can be written as

$$(10) \quad \lim_{\frac{m_c^2}{s}, \frac{m_c^2}{Q^2} \rightarrow 0} \sigma(ep \rightarrow e + J/\psi + X) \rightarrow \int \frac{dQ^2}{Q^2} \int dy \int dx f_{g/p}(x) \delta(xys - Q^2) \times \\ \times \frac{2\alpha_s(Q^2)\alpha^2 e_c^2 \pi^2}{m_c Q^2} \frac{1 + (1-y)^2}{y} \left(\langle \mathcal{O}^{J/\psi} [8, ^1S_0] \rangle + 3 \frac{\langle \mathcal{O}^{J/\psi} [8, ^3P_0] \rangle}{m_c^2} \right),$$

where y is the momentum fraction of the J/ψ relative to the incoming electron. So J/ψ production in DIS directly probes the NRQCD matrix elements $\langle \mathcal{O}^{J/\psi} [8, ^1S_0] \rangle$ and $\langle \mathcal{O}^{J/\psi} [8, ^3P_0] \rangle$, and provides a sensitive test of NRQCD factorisation. At $\mathcal{O}(\alpha\alpha_s^2)$ the J/ψ is produced through 3S_1 colour-singlet and $^1S_0, ^3S_1$ and 3P_J colour-octet configurations. The $\mathcal{O}(\alpha\alpha_s^2)$ colour-octet processes are particularly important at large values of the inelasticity z . Note, however, that the upper endpoint region of the z -distribution in

⁽¹⁶⁾ The same holds in the CDF measurements.

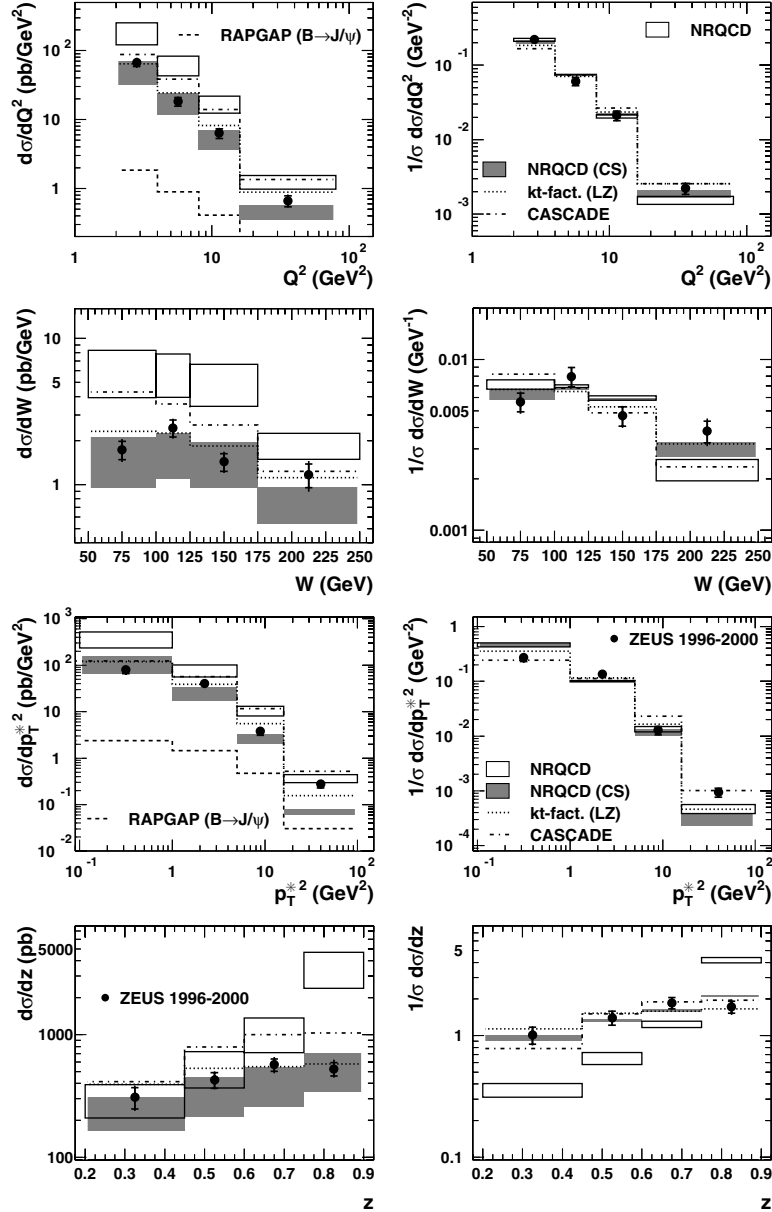


Fig. 3. – Differential cross-sections for the reaction $e p \rightarrow e J/\psi X$ in the kinematic region $2 < Q^2 < 80 \text{ GeV}^2$, $50 < W < 250 \text{ GeV}$, $0.2 < z < 0.9$ and $-1.6 < Y_{\text{lab}} < 1.3$ as a function of Q^2 , W , p_T and z , left panel. The plots on the right show the data and the theoretical predictions normalised to unit area. The inner error bars of the data points show the statistical uncertainty; the outer bars show statistical and systematic uncertainties added in quadrature. The data are compared to the LO NRQCD predictions (CS+CO), light bands, the LO CS calculation, shaded bands, the prediction in the k_T -factorisation approach within the CSM and to the CASCADE MC predictions. In the LZ calculation m_c was set to 1.4 GeV, the renormalisation and factorisation scales were both set equals to k_T for $k_T > 1 \text{ GeV}$ and fixed at 1 GeV for $k_T \lesssim 1 \text{ GeV}$, where for the CASCADE simulation m_c was set to 1.5 GeV, $\alpha_S = \alpha_S((M_\psi^2 + p_T^2)^{1/2})$, and the unintegrated gluon-density parametrisation “J2003 set 2” was adopted. The beauty contribution, estimated using the RAPGAP MC, is also shown separately.

J/ψ leptonproduction cannot be predicted reliably without summing large higher-order corrections in the NRQCD velocity expansion, similar to photoproduction. The theoretical cross-sections include the $\mathcal{O}(\alpha_s^2)$ colour-singlet process as well as the colour-octet contributions.

The inelastic production of J/ψ mesons in ep collisions has been studied with the ZEUS detector [7] using an integrated luminosity of 109 pb^{-1} . The measurements were performed in the kinematic range $2 < Q^2 < 80 \text{ GeV}^2$, $50 < W < 250 \text{ GeV}^2$, $0.2 < z < 0.9$, $-1.6 < y^{\text{lab}} < 1.3$; various other cut were applied in order to ensure a good final state reconstruction, small fake μ , small PHP and elastic/diffractive contaminations and a good removal of large initial state radiation events. The residual diffractive proton-dissociative background⁽¹⁷⁾ was subtracted bin-by-bin from all measured cross-sections according to the EPSOFT MC predictions ($6 \pm 1\%$). A bin-by-bin correction was also applied to tacking into account the geometric acceptance, the detector, trigger and reconstruction inefficiencies, as well as the detector resolution, estimated using the EPJPSI MC generator.

The differential cross-sections as a function of Q^2 , W , p_T^2 and z are shown in fig. 3, together with the predictions of a NRQCD model, the CS calculation with k_T factorisation (LZ) and with the CASCADE MC simulation. The beauty contribution, estimated using the RAPGAP MC, is also shown separately.

The CASCADE calculation overestimates the data, especially the differential cross-section in z for medium-high values of z and as function of Q^2 . This is quite unsuspected, since missing higher-order effects, relativistic corrections (not available for the off-shell matrix element) and colour-octet contributions not accounted by the event generator would bring the MC to underestimate the cross-sections.

Otherwise, the calculations based on the k_T -factorisation describe the data very well, both in shape and normalisation, in spite of the fact that the k_T -dependent parton distributions are not very well known phenomenologically and that there are possibly unresolved theoretical issues, such as the universality of the k_T -dependent parton distributions.

A little surprising is also the fact that the predictions with just the CS process generally agree with the data, whereas the inclusion of CO terms seems to worsen the agreement.

Learning the lesson from the photoproduction results, we expect a better description of the experimental data when NLO calculations will be available also in DIS regime. Actually, the inclusion of higher-order process in the calculations seems to be more important than the CO contributions.

REFERENCES

- [1] ZEUS COLLABORATION, *The ZEUS detector*, edited by HOLM U., Status Report (unpublished), DESY (1993), available on <http://www-zeus.desy.de/bluebook.html>.
- [2] ABBIENDI G. *et al.*, *Nucl. Instrum. Methods A*, **333** (342) 1993.
- [3] CDF Collaboration (ABE F. *et al.*), *Phys. Rev. Lett.*, **79** (1997) 572.
- [4] H1 COLLABORATION, *Eur. Phys. J. C*, **25** (2002) 1,25.
- [5] ZEUS COLLABORATION, *Eur. Phys. J. C*, **27** (2003) 173.
- [6] ZEUS COLLABORATION, submitted to the *International Europhysics Conference on HEP*, 17-23 July 2003, Aachen, Germany-Abstract 569.
- [7] ZEUS COLLABORATION, *Eur. Phys. J. C*, **44** (2005) 13.

⁽¹⁷⁾ Migrate into the data sample due to the finite z resolution.